# CO6-1 Design and Synthesis of Boron-containing Compounds for Effective Accumulaion in Tumor Tissues and Detection by Boron Magnetic Resonance Imaging

S. Aoki[1], T. Tanaka[1], Y. Hisamatsu[1], Y. Sawamoto[1], Rikita Araki[2], Takaomi Saido[3], T. Suzuki[4], K. Horie[4], Ryo Abe[4], S. Masunaga[5], N. Kondo[5], Y. Sakurai[5], and K. Ono[5]

[1]*Faculty of Pharmaceutical Sciences, Tokyo University of Science*
[2] *Bruker Biospin K. K.*
[3] *RIKEN Brain Science Institute*
[4]*Research Institute of Biomedical Sciences, Tokyo University of Science*
[5]*Research Reactor Institute, Kyoto University*

**INTRODUCTION:** Boron neutron capture therapy (BNCT) is one of powerful therapies for local tumor control in the treatment of brain tumor, melanoma, and so on [1]. Our object in this work is to develop new methods for the tumor-specific accumulation of boron-containing compounds and the real-time detection of B concentrations in local tumor tissues. In this study, we have designed and synthesized new boron compounds appended with glucose moiety and metal chelators for BNCT and B NMR (nuclear magnetic resonance) or MRI (magnetic resonance imaging) [2].

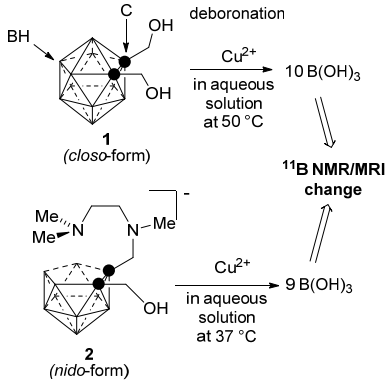


Fig 1. Deboronation reaction of carborane derivatives **1** and **2**, induced by Cu(II) in aqueous solutions.

**EXPERIMENTS and RESULTS:**

**$^{11}$B NMR and MRI change of carborane derivatives by decomposition reaction promoted by copper(II).**

Decomposition reaction of **1** and **2** was by $^{11}$B NMR and MRI. Interestingly, the probe **2** undergoes faster decomposition than that of **1** at 37 °C and neutral pH, which was successfully detected on $^{11}$B NMR and MRI [3,4].

**Concice and versatile synthesis of natural product derivatives that possess B-cluster parts**

Sulfoquinovosyl acylpropanediol (SQAP) has been reported to show a variety of biological activities, including accumulation in tumor cells and the inhibition of tumor cell growth. We developed a new concise and versatile synthesis of SQAP itself and derivatives bearing iodoaryl groups and boronclusters (**5**) starting from compound **3** via the selective acylation at C1 position of the intermediate **4** [5].

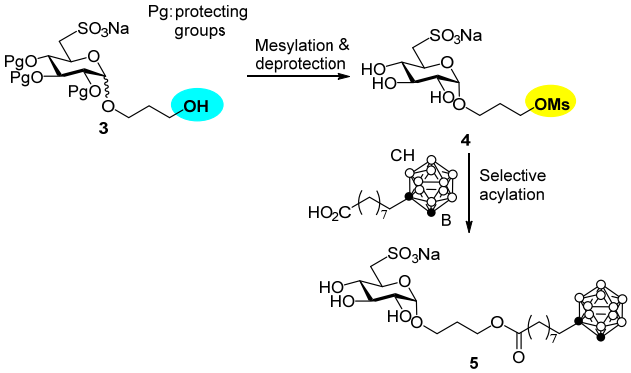


Fig 2. The synthetic route for preparing SQAP derivatives in this study

**Design and synthesis of new carriers of boron-containing compounds.**

The aforementioned results prompted us to design and synthesize new carrier compounds of B-containing compounds. It was found that uptake of the conjugate compounds of our new carriers and B-containing compounds is almost similar to boronylphenylalanine (BPA) (these structures are not shown in this paper, because they will be submitted to the patent in due course).

.

**REFERENCES:**

[1] a) R. F. Barth *et al.*, *Clin. Cancer Res.*, **11** (2005) 3987-4002. b) R. F. Barth et al. *Rad. Oncol.* **7** (2012) 146-166.
[2] a) G. W. Kalbalka, *et al. J. Neuro-Oncol.* **33** (1997) 153-161. b) P. Bendel, *NMR in Biomed.* **18** (2005) 74-82.
[3] T. Tanaka *et al.*, *Eur. J. Inorg. Chem.* 1819-1834 (2016).
[4] T. Tanaka *et al.*, *Eur. J. Inorg. Chem.* 3330-3337 (2016).
[5] T. Tanaka *et al.*, *Chem. Pharm. Bull.* **65**, 566-572 (2017).

# CO6-2 Study of Localization Estimation of Abasic Sites in DNA Irradiated with Ionizing Radiation

K. Akamatsu, N. Shikazono and T. Saito[1]

*Irreparable DNA Damage Analysis Research Group, Quantum Beam Science Research Center, Japan Atomic Energy Agency (JAEA)*
*[1]Research Reactor Institute, Kyoto University*

## INTRODUCTION:

DNA lesions induced by ionizing radiation and chemicals can cause mutation and carcinogenesis. In particular, "clustered damage" site, that is a DNA region with multiple lesions within one or two helical turns, is believed to hardly be repaired. This damage is considered to be induced, *e.g.*, around high-LET ionizing radiation tracks. However, detail of the damage is not known. We have already developed a method for estimating degree of localization of abasic sites (APs) in DNA using Förster resonance energy transfer occurred between different fluorescence probes ("hetero-FRET" using Alexa350 and Alexa488) [1] . The results showed that $^{12}C^{5+}$ beam produced close APs within a track: the apparent distance calculated was approximately 17 base pairs [2]. This finding indicates that *direct radiation effect* of $^{12}C^{5+}$ beam near the Bragg peak produces clustered DNA damage. We have recently applied the method to DNA in a cell-mimetic radical scavenging condition. However, there are some problems of the complex protocol and of the sensitivity due to the low extinction coefficient of Alexa350. We have, therefore, developed "homo-FRET" occurred between two or more Alexa488 molecules. We will obtain magnitude of FRET also from "fluorescence anisotropy" of homo-FRET between Alexa488 molecules. The new protocol using homo-FRET enables us to estimate DNA damage localization without any enzymes and improves sensitivity to detect a clustered damage.

## EXPERIMENTS:

●*Sample preparation and irradiation*

The plasmid DNA digested by Sma I was used (linear form). The DNA was dissolved to be 0.1 g/L in 0.2 M Tris-HCl buffer (pH 7.5) which is a cell-mimetic condition in relation to radical scavenging capacity. Twenty microliters of the DNA solution was transferred to a microtube (0.5-mL size), and was irradiated with $^{60}$Co γ-rays (LET: ~0.2 keV/μm; Kyoto University Research Reactor Institute: KURRI) as a standard radiation source. Moreover, the DNA solution was irradiated with carbon ion beam (LET: ~ 90 keV/μm) at HIMAC (National Institute of Radiological Sciences, QST).

●*Preparation of fluorophore-labeled irradiated DNA and the FRET observation*

The irradiated DNA (10 μL in water) and 10 μL of 100 mM Tris-HCl (pH 7.5) were mixed in a microtube. Two microliters of Alexa488/DMSO was added to the DNA solution and was incubated for 24 h at 35°C. The fluorophore-labeled DNA was purified by ethanol-precipitation followed by ultrafiltration. The fluorescence anisotropy was measured at 525 nm (ex. 470 nm).

The anisotropy, $< r >$, is defined as follows:

$$< r > = \frac{I_{VV} - G \bullet I_{VH}}{I_{VV} + 2G \bullet I_{VH}},$$

where $I_{VV}$ is the fluorescence intensity when the excitation and emission polarizers are both vertically oriented. $I_{VH}$ is one when the excitation/emission polarizers are vertically/horizontally oriented. $G$ is the grating factor defined as $I_{HV}/I_{HH}$.

## RESULTS AND DISCUSSION:

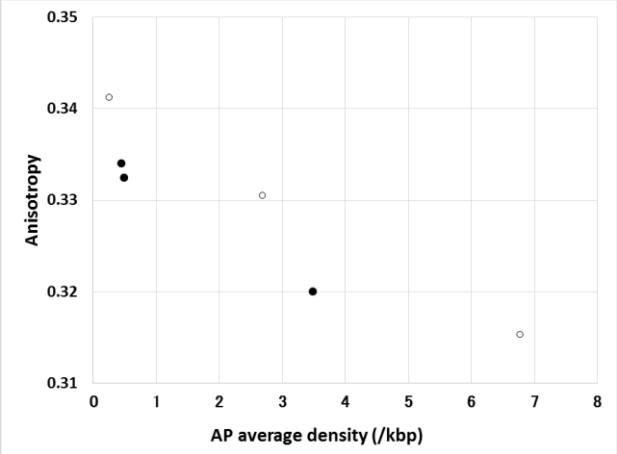


Fig. 1. Relationship between AP average density (the number of APs per kilo base pairs) and fluorescence anisotropy for $^{60}$Co γ-rays (o) and carbon ion beam (HIMAC) (●).

In general, fluorescence anisotropy decreases with increasing FRET [3]. As shown in Fig.1, there was a little difference between the γ-ray data points and a theoretical curve based on exponential distribution. This finding suggest that APs produced by the γ-rays are likely to be localized compared to those randomly distributed. This tendency is similar to the hetero-FRET results as shown previously [2]. A radiation "spur" on or nearby DNA might sometimes produces clustered damage. On the other hand, the anisotropy curve (points) for carbon ion beam was slightly lower than that for the γ-rays, whereas that for carbon ion beam to dry DNA was much lower than these experiment to aqueous DNA (data not shown). This implies that clustered DNA damage mainly occurs by direct radiation effect.

## REFERENCES:

[1] K. Akamatsu, N. Shikazono, Anal. Biochem. **433** (2013) 171-180.
[2] K. Akamatsu, N. Shikazono, and T. Saito, Radiat. Res. **183** (2015) 105-113.
[3] L. W. Runnels, and S. F. Scarlata, Biophys. J. **69** (1995) 1569.

# CO6-3 Age-related Stresses Induce Asp Isomerizations of αA-crystallin in Lens

T. Takata[1,2] and N. Fujii[2]

[1]*Tokyo University of Pharmacy and Life Sciences*
[2]*Research Reactor Institute, Kyoto University*

**INTRODUCTION:** The passive chaperone lens α-crystallin (α-Crys), a small heat shock protein, is composed of two subunits (~ 20 kDa) αA- and αB-crystallin (αA-Crys and αB-Crys), which form a hetero-oligomeric and polydisperse complex with molecular mass of ~ 600 kDa in the vertebrate lenses. Recent studies by LC/MS/MS analysis have shown that many aspartyl residues (Asp) in αA-Crys inverted to isomers (Lβ-Asp, Dα-Asp, Dβ-Asp) with age (1-2). However, it is not well understood whether Asp isomers in native polymeric αA-Crys are different from those in dissociated αA-Crys. In the present study, we examined to clarify the isomerized Asp in dissociated αA-Crys, which may contribute to abnormal lens protein subunit-subunit interactions in aged lens.

**EXPERIMENTS:** Lens of four different ages (42, 54, 69 and 83 years old) were homogenized, centrifuged, and the soluble fraction was applied to size-exclusion chromatography (Fig. 1). The polymeric and monomeric αA-Crys fractions were independently obtained, and then digested by trypsin. Each tryptic peptide was applied to mass spectrometry equipped with nano-scale liquid chromatography to extract each of αA-Crys-derived peptides containing Asp isomers. The ratio of Asp isomers was determined by the comparison of peak area from four Asp isomer containing peptide.

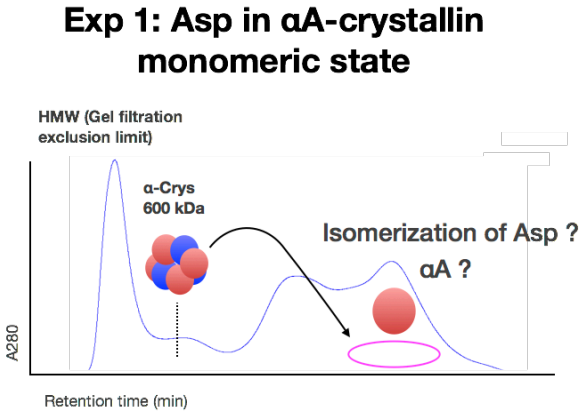


Fig. 1. Experiment design. This is typical size exclusion chromatograms from aged lens soluble fraction. The αA-Crys hetero-oligomer was eluted at early time. The αA-Crys monomeric fraction should be eluted at later in aged lens. Each fraction was measured by absorbance at 280 nm during chromatography, fractionated and applied for D/L analysis independently.

**RESULTS:** αA-Crys was identified as a polymeric and monomeric state in the soluble fraction of aged lens. The isomerization of Asp 58, Asp 84 and Asp 151 of αA-Crys were highly detectable in the monomeric fraction, but not those in the polymeric one. These results showed that the distribution of Asp isomers is different between the dissociated and aggregated states of α-Crys in aged lens. Furthermore, The ratios of Asp isomers at the residues, 58, 84 and 151 in monomeric αA-crystallin were age-dependent and similar to the previously reported ratio in αA-crystallin from the water-insoluble fraction of aged lens (Fig. 2). Thereby, age-dependent Asp isomerization in α-Crys is likely to contribute to the solubility of lens protein in aged lens. Age-dependent isomerization of Asp is also stress dependent. The more damage in lens, the more isomerization would be presented in lens Crys even in the same age. In future study, we will add various stresses into lens Crys such as UV, γ-ray and neutron beam to cause oxidative damage, and quantitated isomerization. From current study, our conclusion is that the isomerization of Asp as well as many other modifications would reduce the normal subunit-subunit interaction of α-Crys with aging, resulting in senile cataract formation.

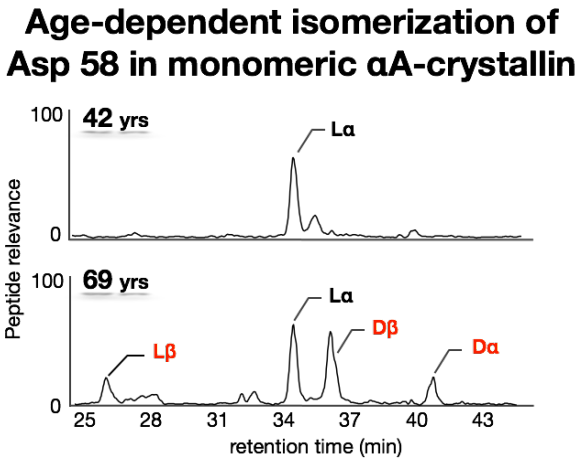


Fig. 2. Age-dependent isomerization of Asp 58 in αAT6 from the monomeric crystallin fraction. The isolated monomeric fraction was further digested by trypsin and applied for LC-MS/MS analysis. Top panel; 42-year-old lens monomeric crystallin fractions. Bottom panel; 69-year-old lens monomeric crystallin fractions.

**REFERENCES:**

[1] N. Fujii *et al.*, J Biol Chem. **287** (2012) 39992-40002.
[2] H, Sakaue, *et al.*, Biochimica et biophysica acta. **1854** (2015), 1-9.

# CO6-4 LC–MS/MS Analysis of Post-translational Modifications of Lens Protein in Patients with Retinitis Pigmentosa

Y. Ikeda, I. Kim[1], S. Nakatake, Y. Murakami and N. Fujii[1]

*Department of Ophthalmology, Graduate School Medical Sciences, Kyushu University*
*[1]Research Reactor Institute, Kyoto University*

**INTRODUCTION:** Retinitis pigmentosa (RP) is a group of inherited retinal degeneration diseases resulting from photoreceptor cell death and are frequently associated with cataract. We previously showed that chronic inflammation plays a role in the pathology of RP and could pose a risk of the development of cataract formation. The aim of this study was to identify the post-translational modifications that occur in lens protein of RP patients during inflammatory process.

**EXPERIMENTS:** Lens samples were collected during cataract surgery. This study was approved by the Institutional Review Board of Kyushu University Hospital (Fukuoka, Japan) and was conducted in accord with the tenets of the Declaration of Helsinki on Biomedical Research Involving Human Subjects. Informed Consent for the research was obtained from all patients. Sample preparation was performed as described in our previous study [1]. Samples were homogenized in 50 mM sodium phosphate buffer (pH 7.4), 150 mM NaCl, 1 mM phenylmethylsulfonyl fluoride (PMSF), 1 mM EDTA by ultrasonication and fractionated into water-soluble (WS) and water-insoluble (WI) fractions by centrifugation at 12,000 × g for 20 min at 4 °C. The WI proteins were dissolved in 8 M urea, and the urea concentration was then diluted to less than 1 M in the same buffer before the enzymatic digestion. The WS proteins were digested with trypsin for 17 h at 37 °C in 50 mM sodium phosphate buffer (pH 7.4), 150 mM NaCl at an enzyme-to-substrate ratio of 1:50 (mol/mol). The WI proteins were digested with trypsin for 17 h at 37 °C in 50 mM sodium phosphate buffer (pH 7.4), 150 mM NaCl, 1 M urea, 1 mM CaCl2 at an enzyme-to-substrate ratio of 1:50 (mol/mol). A nano-flow HPLC system was used for liquid chromatography (LC). Mass spectrometry (MS) was performed on an ion trap system. Peptides (500 ng) resulting from digestion with trypsin were separated by nano-flow HPLC using a C18 column (L-column, 0.1 × 150 mm) with a linear gradient of 5%–60% acetonitrile in the presence of 0.1% formic acid at a flow rate of 0.5 μL/min over 120 min and analyzed by Proteome Discoverer 1.0 software. MS analysis was carried out by alternating between full MS and MS/MS scans. The MS/MS scan used the collision-induced dissociation (CID) mode with dynamic exclusion function.

**RESULTS:** Post-translational modifications including oxidation and deamidation was detected in several lens proteins, such as α- and β-crystallins in patients with RP.

**REFERENCE:**

[1] Kim I, *et al*. Site specific oxidation of amino acid residues in rat lens γ-crystallin induced by low-dose γ-irradiation. Biochem Biophys Res Commun. **466** (2015) 622-628.

# CO6-5 Purification, Crystallization, and X-ray Diffraction Study of Lysozyme in $D_2O$ and $H_2O$ Solution.

T. Chatake, S. Fujiwara[1], I. Tanaka[2]

*Research Reactor Institute, Kyoto University*
*[1] Quantum Beam Science Research Directorate, National Institutes for Quantum and Radiological Science and Technology*
*[2] Faculty of Engineering, Ibaraki University*

**INTRODUCTION:** Neutron scattering length of hydrogen (H) and its isotope deuterium (D) are remarkably different, and such isotope effect is widely utilized in neutron experiments. In particular, the contrast analysis between deuterated and non-deuterated sample is the main method in small angle neutron scattering (SANS) for biology, because H content of biomacromolecule is about half of all atoms in the molecule. In SANS, deuteration is used for labeling arbitrarily a part of macromolecular complex, simultaneously it decrease background noise of neutron scattering. In previous studies, we developed deuterium/hydrogen (D/H) contrast technique for neutron protein crystallography (NPC) [1]. This technique has great advantages in determining and evaluating hydrogen atoms, especially, it is very powerful for visualizing water molecules ($D_2O$/$H_2O$) surrounding proteins. The hydration structure is very important for folding and function of protein. In order to compare hydration structures of various kinds of proteins, we are crystallizing the proteins and carried out preliminary diffraction studies using X-ray.
Here, we report purification, crystallization, and X-ray diffraction study of lysozyme in $D_2O$ and $H_2O$ solution.

**EXPERIMENTS:** Hen egg white lysozyme (Sigma Aldrich) was purified prior to crystallization. 100 mg lysozyme power was solved in 3 mL of 50 mM sodium acetate (NaAc) buffer (pH5.0). The lysozyme solution was 0.22 mm-filtered, and then applied on GE Hiscreen CatopSP Impres ion-exchange column (CV:4.7 mL), lysozyme was eluted by graduation from 0 M to 1 M NaCl in the 50 mM NaAc buffer (pH 5.0). The eluted lysozyme solution was dialyzed against 50 mM NaAc buffer (pH 4.5) overnight, and then concentrated to be 40 mg/mL by centrifuge concentration.
Crystallization for preliminary X-ray diffraction experiment was carried out sitting drop vapor diffusion method. Reservoir solutions contained 0.8, 1.0, or 1.2 M NaCl in the NaAc buffer (pH4.5). Each droplet was prepared by mixing 20 μL of 40 mg/mL lysozyme solution and 20 μL of reservoir solution. Crystallization plates were stored at 20 °C. The same crystallization was performed using $D_2O$ solution, in which deuteration was carried out the repeats of buffer exchange from $H_2O$ buffer to $D_2O$ buffer.
Preliminary X-ray diffraction experiments were carried out at beamline NW12 of the synchrotron facility in Photon Factory. Deuterated and non-deuterated crystals were sealed in glass capillaries with each buffer, respectively, and synchrotron experiments were carried out at room temperature (300K). X-ray diffraction images were collected by the helical scanning method in order to avoid serious radiation damage on the crystals. 200 oscillation images were taken with $\Delta\omega = 1°$ and t = 1 sec. Since considerable numbers of low-resolution diffractions were saturated on the detector, two data sets were taken for each of $D_2O$- and $H_2O$-crystals with and without attenuator. Diffraction spots on the images were indexed, integrated, and merged by the program HKL2000.

**RESULTS:** After two weeks one or few large crystals emerged in droplets with the reservoir solution of 0.8 or 1.0 M NaCl. The side-length of these crystals were at least larger than 0.7 mm, and sometimes larger than 1.0 mm. In the present study, purification process seems to improve crystal size of lysozyme.

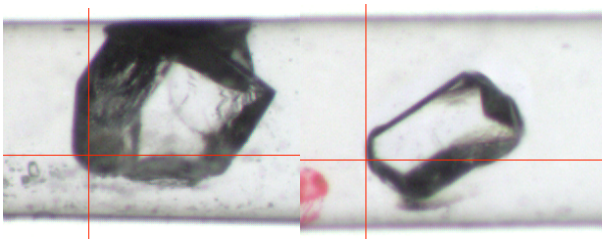

Fig. 1. Lysozyme crystal used for X-ray experiments. H2O-crystal (right) and D2O-crsytal (left) was sealed in a capillary with a diameter of ~ 1 mm.

Both crystals belong to the same space group $P4_32_12$, with the similar cell dimensions (a=b=79.2 Å, c=38.0 Å for $H_2O$ crystal, a=b=79.2 Å, c=37.9 Å for the $D_2O$ crystal), suggesting the isomorphousness between the two crystals. For the $H_2O$ crystal, 1.35 Å X-ray data could be obtained with the completeness and $R_{merge}$ of 99.9% and 6.9%, respectively. Meanwhile, for the $D_2O$ crystal, 1.45 Å X-ray data could be obtained (completeness and $R_{merge}$ were 99.8% and 6.90%). In order to compare the two crystal structures, structure determinations are in progress.

**REFERENCE:**
[1] T. Chatake and S. Fujiwra, Acta Crystallogra. D72 (2016) 71-82.

# CO6-6 Measurement of Transmittance Spectra of a Cryo-Sectioned Tissue of Brain Tumor C6 Model in the Sub-Terahertz Reagion-IV

T. Takahashi and N. Miyoshi[1]

*Research Reactor Institute, Kyoto University*
*[1] National University of Kyoto Institute of Technology*

**INTRODUCTION:** The accelerator-based radiation source in the millimeter and terahertz wave region has very attractive feature for the spectroscopy. Coherent transition radiation (CTR), which has been emitted from the short bunches of electrons at the KURRI-LINAC, has been used to observe the transmittance spectra of a sectioned tissue of raw brain tumor C6 model as a collaborate study in the research reactor institute, Kyoto university. The absorption spectra in the sub-terahertz region had been not so clear for the raw tumor tissue although Ashworth-PC. *et al*. [1] had reported for the excised human breast cancer by a terahertz pulsed spectroscopy observed at 320 GHz, which was estimated a longer relaxation time component of the induced electricity for water molecules [2-3] in the raw tumor tissue for three years at the linear analysis.

We also estimated what kind of water molecules become dominant in the viable and necrotic cancer regions by the different measurement method as an aim of 2D mapping study.

**EXPERIMENTS:** **(1)** Instrument of Near-field in tera-hertz region: The experiment was performed at the coherent radiation beamline [4] at the 40-MeV L-band linac of the Research Reactor Institute, Kyoto University. The THz-wave source was CTR emitted from an aluminum foil with 15-μm thickness. The radiation was detected by a liquid helium cooled Si bolometer. The conical cone with an aperture 260 μm in diameter was used as the illumination probe and its F-number was 2.5. The spectrum of CTR was measured by a Martin-Puplett type interferometer.

**(2)** Sample preparation: A cryo-sectioned (thickness=100 μm) tissue was prepared from the raw C6 glial tumor model using a Cryo-section (C) Maker (Leica) and was sealed sandwich-type with polyvinylidene chloride (PVDC) film (thickness=10 μm), under freezing condition (-20 C) before the measurements. The rest large block of the tumor tissue was fixed with 10% formaldehyde for 1 week and was made of paraffin block to slice of 50 μm film sample (P) with PVDC film.

**RESULTS:** The absorbance of the raw tissue at 16 $cm^{-1}$ was larger than 0.1 comparing the paraffin sample which was decreased of water contents by formaldehyde effect as shown in Figs. 1 and 2. Especially, the water contents were distributed in the necrotic area (white area in cryo-section). On the other hand, the absorbance at 19 $cm^{-1}$ was distributed also in the necrotic area of the tumor tissues which looks like paraffin contents (lipid). In conclusion, lipid and water contents were distributed lich in the necrotic area of tumor tissue by this sub-THz LINAC beam analysis. It was found the absorbance at 16 and 19 $cm^{-1}$ were belonged as the water and lipid components, respectively in tumor tissue. The condition of water components should be more cleared in future, a cluster model of the water molecules and the other absorbance in this sub-THz region.

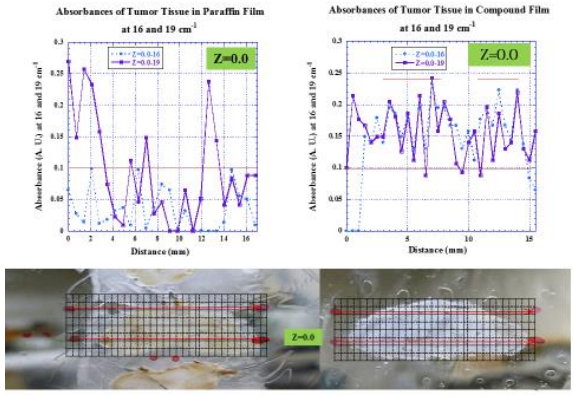


Fig. 1 Linear analysis of Cryo (C) and Paraffin (P) -sectioned samples.

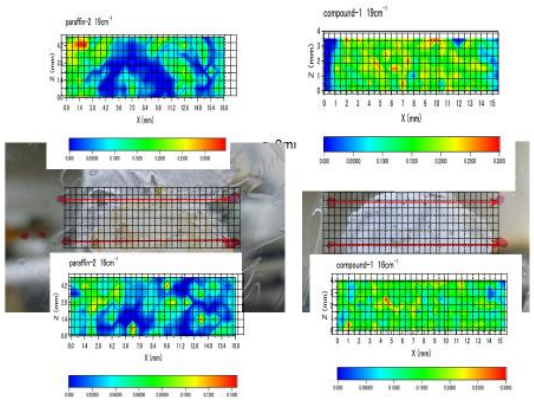

Fig. 2 2D-Mapping Images of Cryo- and Paraffin-sectioned samples at 16 and 19 $cm^{-1}$, respectively.

**REFERENCES:**

[1] Phillip C. Ashuworth, *et. al*., *Optics Express*, **17(14):** 12444-12454 (2009).
[2] Toshiko Fukasawa, *et al*., *Phys. Rev. Let.*, **95:** 197802 (2005).
[3] Hiroyuki Yada, *et al*., *Chem. Phys. Let.*, **464:** 166-170 (2008).
[4] T. Takahashi, *et al.*, Rev. Sci. Instrum. **69** (1998) 3770.

# CO6-7 The Study for Development and Application of Tissue Equivalent Neutron Dosimeter

M. Oita, T. Kamomae[1], T. Takada[2] and K. Sakurai[2]

*Graduate School of Health Sciences, Okayama University*

*[1] Graduate School of Medicine, Department of Radiology, Nagoya University*

*[2]Research Reactor Institute, Kyoto University*

**INTRODUCTION:** Recent years, the clinical application of boron neutron capture therapy (BNCT) has been expected to make significant contributions to treatment for intractable cancer such as glioblastoma multiforme and melanoma. In BNCT, the boron (n,α)-reaction of the isotope $^{10}B$ has a high cross section toward thermal neutrons, and the produced alpha and lithium particles have a short range on the micrometer scale. However, the neutron spectrum always spans a broad energy range, which results in different dose components and biological effects in tissue. Therefore, there are some difficulties of neutron dosimetry in clinical practice.

A radiochromic film (RCF) is one of the most useful devices for the QA of radiotherapy equipment. The advantages of RCFs are their high spatial resolution, small energy dependence, tissue equivalence, and self-development without processing in a darkroom[1]. A reflective-type RCF, e.g., GAFCHROMIC® EBT3, has been developed for qualitative dosimetry such as stereotactic irradiation (STI) and intensity modulated radiotherapy (IMRT)[2,3]. In this work, the authors investigated the response of reflective-type RCF for neutron beam as a tissue equivalent dosimeter.

**EXPERIMENTS:** A reflective-type RCF, GAFCHROMIC® EBT3 (Ashland Inc., Wayne, NJ, USA) using an Americium–Beryllium ($^{241}$Am–Be) neutron source (74 GBq, $5\times10^6$ neutrons.s-1) with a cylindrical design (20 mm diameter by 30 mm long) made of the corrosion-resistant alloy was evaluated in this study. The RCFs were handled by the recommendation outlined in the American Association of Physicists in Medicine Task Group No. 55 report[1].

For irradiation, 6.0 × 6.0 $cm^2$ pieces of the RCF were placed at 1 cm, 4 cm, and 7 cm from just beneath the source with slit window along one direction, and with behind 1 mm acrylic plate along opposite direction in air (Fig.1). The RCF pieces were irradiated 180 min by the source, respectively.

**RESULTS:** Fig.1 shows the geometry of irradiation of RCFs by the $^{241}$Am-Be neutron source. Fig.2 shows the change of pixel values of RCFs irradiated by the $^{241}$Am–Be neutron source. There was significance difference of pixel values of irradiated RCFs by the neutron source. The change of pixel value of RCF piece between 1 cm and 4 cm was 1811, while the value with the acrylic plate was attenuated by 1513. The dose in former converted by X-ray calibration of the RCF in the air were 36.2 cGy. Similarly, the dose of using a NaI scintillation survey meter was 15.3 cGy. Besides neutrons, the RCFs were exposed to gamma rays coming from events taking place in the source itself and the surrounding moderator. Further analysis was needed of the response of RCFs with neutron spectrum and contributions of gamma rays using Monte Carlo simulation. However, the results suggested that the dosimetry using RCFs is important for a better knowledge of fast neutron flux distribution with the $^{241}$Am–Be source. Moreover, it would be feasible for BNCT dosimetry in medical application.

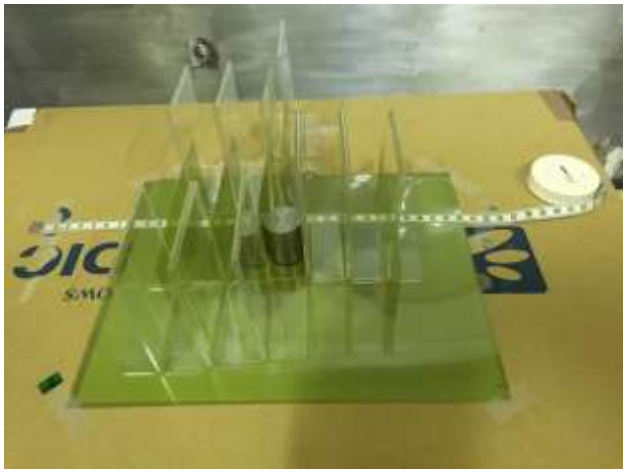

Fig. 1. The geometry of irradiation of RCFs by the $^{241}$Am-Be neutron source.

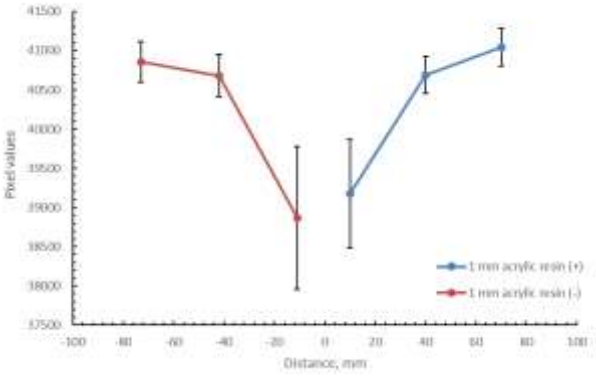


Fig. 2. The change of pixel values of the RCFs irradiated by the $^{241}$Am-Be neutron source.

**REFERENCES:**

[1] Niroomand-Rad, Azam, *et al*. Medical physics **25** (1998), 2093-2115.

[2] Borca, Valeria Casanova, *et al*. Journal of applied clinical medical physics **14** (2013).

[3] Fiandra, Christian, *et al.* Medical physics **40** (2013).